PROCEEDINGS OF SCIENCE

S-wave contribution to rare $D^0 \to \pi^+\pi^-\ell^+\ell^-$ decays in the Standard Model and sensitivity to New Physics

Luiz Vale Silva,[a,*] **Svjetlana Fajfer**[b] **and Eleftheria Solomonidi**[a]

[a] *Departament de Física Teòrica, Instituto de Física Corpuscular, Universitat de València – Consejo Superior de Investigaciones Científicas, Parc Científic, Catedrático José Beltrán 2, E-46980 Paterna, Valencia, Spain*

[b] *Jožef Stefan Institute, Jamova 39, P. O. Box 3000, 1001 Ljubljana, Slovenia, Faculty of Mathematics and Physics, University of Ljubljana, Jadranska 19, 1000 Ljubljana, Slovenia*

E-mail: luizva@ific.uv.es, svjetlana.fajfer@ijs.si, elefsol@ific.uv.es

Physics of the up-type flavour offers unique possibilities of testing the Standard Model (SM) compared to the down-type flavour sector. Here, we discuss SM and New Physics (NP) contributions to the rare charm-meson decay $D^0 \to \pi^+\pi^-\ell^+\ell^-$. In particular, we discuss the effect of including the lightest scalar-isoscalar resonance in the SM picture, namely, the $f_0(500)$, which manifests in a big portion of the allowed phase space. Other than showing in the total branching ratio at an observable level, the $f_0(500)$ resonance manifests as interference terms with the vector resonances, such as at high invariant mass of the leptonic pair in distinct angular observables. Recent data from LHCb optimize the sensitivity to P-wave contributions, that we analyse in view of the inclusion of vector resonances. We propose the measurement of alternative observables which are sensitive to the S-wave and are straightforward to implement experimentally. This leads to a new set of null observables, that vanish in the SM due to its gauge and flavour structures. Finally, we study observables that depend on the interference of the S-wave with generic NP contributions from semi-leptonic four-fermion operators.

The European Physical Society Conference on High Energy Physics (EPS-HEP2023)
21-25 August 2023
Hamburg, Germany

*Speaker

PoS(EPS-HEP2023)353

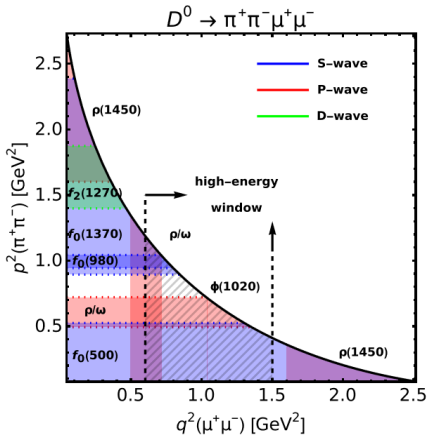

Figure 1: Phase space allowed in the decay $D^0 \to \pi^+\pi^-\mu^+\mu^-$; the invariant mass of the pion (muon) pair is denoted p^2 (respectively, q^2). Some scalar (**blue**), vectorial (**red**) and tensorial (**green**) resonant contributions are shown; the bands correspond to $(m \pm \Gamma/2)^2$. The "high-energy window" referred to in the plot corresponds to $m^2_{\rho^0} \lesssim q^2 \lesssim 1.5$ GeV^2, for which only $f_0(500)$ gives an important contribution among the S-wave contributions, and is indicated by a hashed pattern delimited by dashed vertical lines.

Flavour Changing Neutral Currents (FCNCs) in the charm sector provide complementary information to analogous down-type transitions (e.g., rare kaon and bottom-meson decays). The biggest difference in here is that the Glashow-Iliopoulos-Maiani (GIM) mechanism is more effective, since in one-loop diagrams the internal flavour cannot be the top quark, but instead the heaviest flavour is the bottom. Together with the hierarchical structure of the Cabibbo-Kobayashi-Maskawa (CKM) matrix, it implies that hadronic effects are very important in the charm sector. Such hadronic effects have to be taken into account in order to match the level of precision reached by data. As we will see, present data allows an improved understanding of the SM contributions. With an improved description of the SM part, it is then possible to achieve cleaner tests of NP contributions.

Noteworthy, there is a rich dataset on multiple different categories of observables already available, that will be obviously enlarged by future LHCb data. The latest LHCb analysis [1] provides bins of the branching ratio with respect to the invariant mass of the di-hadron and lepton pair. Not surprisingly, resonances are seen in $D^0 \to \pi^+\pi^-\mu^+\mu^-$ and $D^0 \to K^+K^-\mu^+\mu^-$ data, such as the ρ^0 (or the ϕ) in the differential distribution with respect to the pion (or the kaon, respectively) pair invariant mass; also, the ρ^0, ω, and ϕ in the differential distribution with respect to the lepton pair invariant mass (the latter ϕ is not allowed in the kaon mode due to phase space restriction). There are also bins of angular observables with respect to the lepton pair invariant mass, that are built in a way to optimize the effect of the P-wave of the pion pair, in $C\mathcal{P}$-symmetrized and $C\mathcal{P}$-asymmetric combinations.

On the other hand, there is no sizable contribution from the SM from short-distance physics, i.e., from local semi-leptonic operators, which is due to the aforementioned GIM mechanism and CKM diagonal structure. The set of effective interactions is the following:

$$\mathcal{H}_{\text{eff}} = \frac{G_F}{\sqrt{2}} \left[\sum_{i=1}^{2} C_i(\mu) \left(\lambda_d Q_i^d + \lambda_s Q_i^s \right) - \lambda_b \left(C_7(\mu) Q_7 + C_9(\mu) Q_9 + C_{10}(\mu) Q_{10} \right) \right] + \text{h.c.} \quad (1)$$

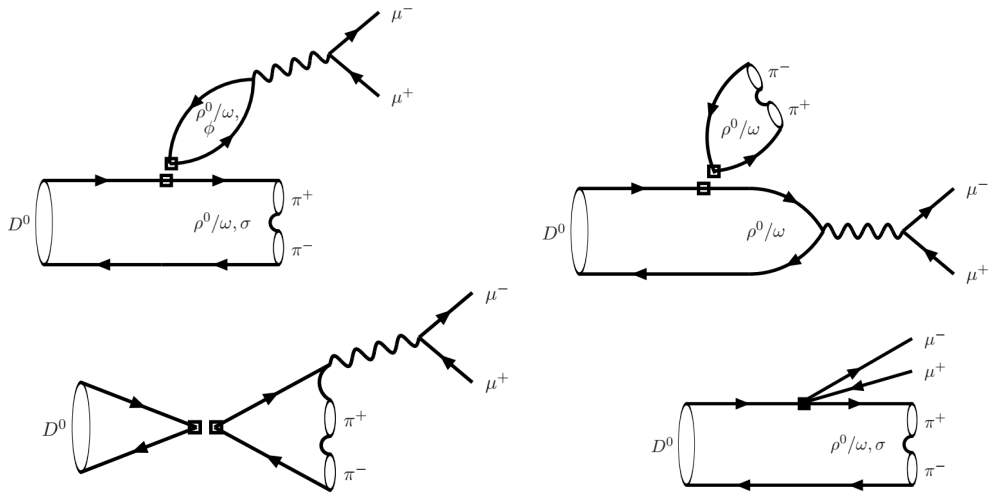

Figure 2: Quasi two-body topologies; the lepton (pion) pair comes from electromagnetic (respectively, strong) decays of the intermediate resonances; (Top, Left) W-type factorization contribution, (Top, Right) J-type factorization contribution, (Bottom, Left) A-type factorization contribution; empty squares represent the two quark colour-neutral bilinears that are factorized. (Bottom, Right) Contributions for which the lepton pair comes from an effective semi-leptonic contact interaction, represented by a solid square.

where $\lambda_q = V_{cq}^* V_{uq}$, with $q = d, s, b$, and

$$
\begin{aligned}
&Q_1^q = (\overline{q}c)_{V-A}(\overline{u}q)_{V-A}\,, \quad Q_2^q = (\overline{q}_j c_i)_{V-A}(\overline{u}_i q_j)_{V-A} \overset{Fierz}{=} (\overline{u}c)_{V-A}(\overline{q}q)_{V-A}\,,\\
&Q_7 = \frac{e}{8\pi^2} m_c \overline{u}\sigma_{\mu\nu}(\mathbf{1}+\gamma_5)F^{\mu\nu}c\,,\\
&Q_9 = \frac{\alpha_{em}}{2\pi}(\overline{u}\gamma_\mu(\mathbf{1}-\gamma_5)c)(\overline{\ell}\gamma^\mu\ell)\,, \quad Q_{10} = \frac{\alpha_{em}}{2\pi}(\overline{u}\gamma_\mu(\mathbf{1}-\gamma_5)c)(\overline{\ell}\gamma^\mu\gamma_5\ell)\,.
\end{aligned}
\tag{2}
$$

In particular, the Wilson coefficient C_{10} is very small, being generated at higher order in electroweak interactions. In order to unveil the short-distance dynamics (e.g., set bounds on NP based on null tests), we need a good description of the long-distance part, resulting from insertions of the current-current operators Q_2^q, $q = d, s$, which is the focus of this work. In particular, we focus on the description of the S-wave, which is done here for the first time in the present context.

The allowed phase space in charm-meson decays is heavily populated with resonance peaks and their tails. This is illustrated in Fig. 1; we have already mentioned the effects of the vector meson resonances ρ^0, ω, and ϕ. Other resonances are also indicated in the figure, such as a tower of scalar-isoscalar resonances, including the well-known $\sigma \equiv f_0(500)$, which is a broad resonance manifesting in $\pi\pi$ rescattering, as well as other P- and D-waves. Here, these resonances will be taken into account via quasi-two body (Q2B) topologies, in which the charm-meson leads to a pair of resonances via weak interactions, which decay electromagnetically to a pair of charged leptons, or via strong interactions to a pair of pions. Moreover, we focus on the lightest resonances, which are better known, and populate a larger fraction of the phase space.

We employ factorization for the description of the Q2B topologies resulting from insertions of operators from the set of effective interactions in Eq. (1). There are four categories of contributions,

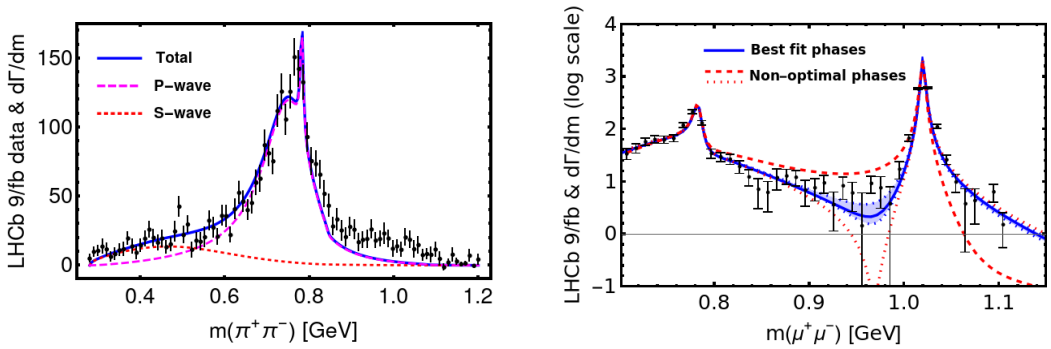

Figure 3: (Left) The prediction for the differential decay rate $d\Gamma/dm(\pi^+\pi^-)$ and LHCb data over the di-hadron invariant mass $m(\pi^+\pi^-)$. The contributions from the S-wave (dotted red) and the P-wave (dashed magenta) add up to the full resonant contribution (solid blue). (Right) The differential decay rate $d\Gamma/dm(\mu^+\mu^-)$ and LHCb data over the di-lepton invariant mass $m(\mu^+\mu^-)$ (logarithmic scale).

which are shown in Fig. 2. They are called W, J, A topologies, and the one resulting from insertions of local semi-leptonic operators that we can neglect in the SM. In bottom-meson physics the most important topology is the W-type, while the J-type is CKM suppressed; in the present context, however, they both contribute at the same level. The A-topology can be neglected since it is proportional to light quark masses, see Ref. [2]. The required non-perturbative inputs are decay constants, form factors, and line-shapes of the intermediate resonances. When fitting LHCb data, this picture has to be extended, to take into account to some extent effects beyond naive factorization, namely, we introduce normalization coefficients and extra strong phases (i.e., beyond the ones of the line-shapes), aiming to model the rescattering between the intermediate resonances.

Moving to fits of the available data, we start with the differential branching ratio as a function of the di-pion invariant mass. With respect to the P-wave, apart from the ρ^0 there is also a small contribution from the ω (which is small because it violates isospin), for which one has to adjust a relative strong phase. More important for this work, there is a clear contribution of the S-wave, more specifically the σ, which being a broad resonance does not manifest as a peak, but as a contribution that spans a large interval of di-pion invariant masses, see the left panel of Fig. 3. This contribution is sizable, and similar in size to the level of S-wave from the σ seen in the analogous non-rare semi-leptonic decay $D^+ \to \pi^+\pi^- e^+\nu_e$ by BESIII [3] (which is 25% therein). There is a poor comparison to data at the upper tail, which is outside the high-energy region defined in Fig. 1, likely to be due at least in part to other resonances.

Having a model for the S- and P-waves of the pion pair, we move to the differential branching ratio as a function of the invariant mass of the lepton pair. First of all, we see clearly in the right panel of Fig. 3 the ρ^0, ω, and ϕ resonances. By exploiting the available data, one can extract differences of strong phases among pairs of resonances, on which the SM predictions depend. These strong phases manifest more clearly in this figure in the regions in between the $\rho^0 - \phi$ resonances, and above the ϕ resonance; the region around the $\rho^0 - \omega$ resonances is also important to constrain a distinct set of strong-phase differences. The solid blue curve corresponds to the best fit situation; as clearly seen, strong-phase configurations corresponding to the dotted or dashed red lines are excluded, i.e., LHCb data can constrain strong-phase differences.

$\frac{\int\langle I_i\rangle^r_+}{\Gamma^r}$	S_1	S_2	S_3	**4**	**5**	S_6	**7**	**8**	S_9
	○	○	×	✓	✓	×	✓	✓	×
SM					0	0	0		~ 0

$\frac{\int\langle I_i\rangle^r_-}{\Gamma^r}$	**1**	**2**	S_4	S_5	S_7	S_8
	✓	✓	×	×	×	×
SM				0	0	~ 0

Table 1: Set of angular observables based on the decay processes $D^0 \to \pi^+\pi^-\mu^+\mu^-$ and $D^0 \to K^+K^-\mu^+\mu^-$. The notation Γ^r stands for the branching ratio in a particular q^2-bin denoted r; $\int\langle I_i\rangle^r_\pm$, $i = 1,\ldots,9$, correspond to different kinds of integration over the angle θ_π, where I_i are the coefficients of the fully differential branching ratio. Cases indicated by S_i, $i = 1,\ldots,9$, have already been measured by LHCb, while cases indicated in boldface are straightforward to implement and probe the S-wave interference with the P-wave. We indicate cases that vanish in the SM, configuring null tests of it (S_7, S_8 and S_9 are suppressed in naive factorization); cases $\{\mathbf{5},\mathbf{7}\}$ are novel null tests of the SM, being based on the S-wave contribution.

Having discussed the differential branching ratios, we now move to a different category of observables. According to the way in which angular observables are defined, one can build combinations that depend or not on the S-wave. In Tab. 1, cases marked with a red cross (×) do not depend on the S-wave, which are the cases that have been measured by LHCb. There are also measured cases that depend on the S-wave, but not through its interference with the P-wave, indicated with a green circle (○). An alternative definition of the angular observables already measured by LHCb, that is straightforward to implement experimentally, would instead depend on the S- and P-waves interference, which is indicated with green ticks (✓). Concerning the predictions for the observables that have already been measured by LHCb, we observe that some quantities are of the order of about 10% in the SM, which are the cases for S_2, S_3, and S_4; their exact definitions are spelled out in Ref. [4]. On the other hand, S_5, S_6, and S_7 vanish in the SM to a very good degree, being then null tests since they require NP contributions [5]. The latter S_7 as well as S_8 and S_9 are close to zero since they correspond to the relative strong phase among P-waves, which is small in naive factorization when considering only the ρ^0/ω. The $\mathcal{CP}$ asymmetries are suppressed because the level of $\mathcal{CP}$ violation in the SM is small. It is interesting that LHCb data sees a similar pattern of values in $\mathcal{CP}$-symmetric and -asymmetric quantities; however, both experimental and theoretical uncertainties are sizable and of the order of a few percent, preventing a better test of the SM.

Also note that binned observables defined in a distinct way could provide distinguished signs of the S-wave contribution, through its interference with the P-wave, such as cases $\{\mathbf{1},\mathbf{2},\mathbf{4},\mathbf{8}\}$ in Tab. 1. This is also illustrated by the differential branching ratio as a function of $\cos(\theta_\pi)$, where θ_π is the angle describing the orientation of the pion pair. Indeed, when only the P-wave is present, this distribution is symmetric with respect to $\cos(\theta_\pi) = 0$, and in presence of the S-wave an asymmetry is produced. The prediction for this observable depends on one extra relative strong phase that is not probed by the differential branching ratios analyzed before. Let us however point out that a clear asymmetry is seen in the non-rare semi-leptonic decay $D^+ \to \pi^+\pi^- e^+\nu_e$ by BESIII [3]; also, in the Cabibbo-allowed mode $D^+ \to K^-\pi^+e^+\nu_e$ by BaBar [6].

Finally, let us cover briefly NP contributions. First of all, limits on NP Wilson coefficients can be probed in different complementary ways, for instance C_{10} can be probed by rare decays $D^0 \to \mu^+\mu^-$, which has been recently improved by LHCb [7], resulting in $|V_{ub}V^*_{cb}C^{(\prime)}_{10}| < 0.43$ @ 95% C.L. (primed operators carry a flipped chirality); a similar bound is achieved by searches of NP contact interactions manifesting in $pp \to \mu^+\mu^-$ [8]. In presence of NP, one can have sizable values

for the angular observables S_5 and S_6 measured by LHCb (the observable S_7 remains small even in the presence of NP in naive factorization), which can reach a few percent when saturating the previous upper bound from rare leptonic decays. A similar comment holds in the case of analogous S- and P-waves interference observables (namely, cases $\{\mathbf{5}, \mathbf{7}\}$ in Tab. 1), which also reach a few percent, thus providing complementary information about tests of NP.

To conclude, we have discussed new LHCb data [1], whose analysis needs improved theoretical models. One has to deal with resonances since the phase space is highly populated by them. Our inclusion of the S-wave improves the description of SM contributions; we provide predictions for new observables sensitive to the S-wave, that are straightforward to be measured by LHCb. In particular, with the S-wave one can formulate novel and complementary null tests of the SM.

Acknowledgements. This work has been supported by MCIN/AEI/10.13039/501100011033, grants PID2020-114473GB-I00 and PRE2018-085325, and by Generalitat Valenciana, grant PROMETEO/2021/071. This project has received funding from the European Union's Horizon 2020 research and innovation programme under the Marie Sklodowska-Curie grant agreement No 101031558. S. F. acknowledges the financial support from the Slovenian Research Agency (research core funding No. P1-0035). L. V. S. is grateful for the hospitality of the Jožef Stefan Institute and the CERN-TH group where part of this research was executed.

References

[1] Roel Aaij et al. Angular Analysis of $D^0 \to \pi^+\pi^-\mu^+\mu^-$ and $D^0 \to K^+K^-\mu^+\mu^-$ Decays and Search for CP Violation. *Phys. Rev. Lett.*, 128(22):221801, 2022. arXiv:2111.03327, doi:10.1103/PhysRevLett.128.221801.

[2] Manfred Bauer, B. Stech, and M. Wirbel. Exclusive Nonleptonic Decays of D, D(s), and B Mesons. *Z. Phys. C*, 34:103, 1987. doi:10.1007/BF01561122.

[3] Medina Ablikim et al. Observation of $D^+ \to f_0(500)e^+\nu_e$ and Improved Measurements of $D \to \rho e^+\nu_e$. *Phys. Rev. Lett.*, 122(6):062001, 2019. arXiv:1809.06496, doi:10.1103/PhysRevLett.122.062001.

[4] Svjetlana Fajfer, Eleftheria Solomonidi, and Luiz Vale Silva. Work in progress.

[5] Stefan De Boer and Gudrun Hiller. Null tests from angular distributions in $D \to P_1P_2l^+l^-$, $l = e, \mu$ decays on and off peak. *Phys. Rev. D*, 98(3):035041, 2018. arXiv:1805.08516, doi:10.1103/PhysRevD.98.035041.

[6] P. del Amo Sanchez et al. Analysis of the $D^+ \to K^-\pi^+e^+\nu_e$ decay channel. *Phys. Rev. D*, 83:072001, 2011. arXiv:1012.1810, doi:10.1103/PhysRevD.83.072001.

[7] R. Aaij et al. Search for Rare Decays of D0 Mesons into Two Muons. *Phys. Rev. Lett.*, 131(4):041804, 2023. arXiv:2212.11203, doi:10.1103/PhysRevLett.131.041804.

[8] Javier Fuentes-Martin, Admir Greljo, Jorge Martin Camalich, and José David Ruiz-Alvarez. Charm physics confronts high-p_T lepton tails. *JHEP*, 11:080, 2020. arXiv:2003.12421, doi:10.1007/JHEP11(2020)080.